Microwave heating of water, ice, and saline solution: Molecular dynamics study

Motohiko Tanaka and Motoyasu Sato
Coordinated Research Center, National Institute for Fusion Science, Toki 509-5292, Japan

(Received 28 July 2006; accepted 9 November 2006; published online 18 January 2007)

In order to study the heating process of water by the microwaves of 2.5–20 GHz frequencies, the authors have performed molecular dynamics simulations by adopting a nonpolarizable water model that has fixed point charges on a rigid-body geometry. All runs are started from the equilibrated states derived from the $\mathbf{I}_c$ ice with given density and temperature. In the presence of microwaves, the molecules of liquid water exhibit rotational motion whose average phase is delayed from the microwave electric field. Microwave energy is transferred to the kinetic and intermolecular energies of water, where one-third of the absorbed microwave energy is stored as the latter energy. The water in ice phase is scarcely heated by microwaves because of the tight hydrogen-bonded network of water molecules. Dilute salt water is significantly more heated than pure water because of the field-induced motion of salt ions, especially that of large-size ions, by the microwave electric field and energy transfer to water molecules by collisions. © *2007 American Institute of Physics*. [DOI: 10.1063/1.2403870]

I. INTRODUCTION

It is well known that microwaves (300 MHz–300 GHz range) can heat solid, liquid, and gaseous matters such as engineering materials, laboratory plasmas, and biological matters including living cells. A microwave oven used in daily food processing is one of such applications. However, unlike laser lights whose photon energy is from several to tens of eV, the photon energy of microwaves is as small as $h\nu \sim 10^{-5}$ eV, and their period is by orders of magnitude longer than the electronic processes (a few femtoseconds) occurring in molecules. Nevertheless, microwaves can control chemical reactions, synthesize organic and inorganic materials,[1,2] and sinter metal oxides with high energy efficiency.[3] Thus, for the microwave-related heating and reactions to take place, nonresonant interactions between waves and materials that persist for many wave periods are expected.

The physical and chemical properties of matters are the basis of materials science, engineering, and biological applications. Especially, the dielectric permittivity was measured extensively as the function of electromagnetic wave frequency and temperature,[4] and precise experimental formulas were presented for the dielectric properties of water, including enhanced heating of salty water.[5] The imaginary part of the dielectric permittivity is related to the energy absorption by dielectric medium, which is termed as *dielectric loss*. For water, the rotational relaxation of permanent electric dipoles occurs approximately in 8 ps at 25 °C (frequency of 120 GHz).[6] For the microwaves less than and around this frequency, only translational and rotational motions of polar molecules are expected to respond to the waves.

The diffusion coefficients and dielectric relaxation properties of water, i.e., the response of electric dipoles to a given initial impulse, were studied theoretically.[7] Numerically, the melting temperature of ice was estimated with several water models.[8] The heating and diffusion of water under high-frequency microwaves and infrared electromagnetic waves were investigated by molecular dynamics simulations using elaborated point-charge models that incorporated either charge polarization or molecular flexibility for the system of 256 water molecules.[9–11] Precise studies showed that the polarizable water model TIP4P-FQ combined with the Lekner method gives more accurate results than fixed-charge model, including the potential energy, dipole moment, dielectric constant, and relaxation times.[12]

The polarizable TIP4P-FQ model needs slightly more computation times, 1.38 and 1.27 times more than the SPC model when the Lekner and Ewald methods are used, respectively, for 256 water molecules.[12] However, the Lekner method requires 2.6 and 2.9 times more computation times than the Ewald method for TIP4P-FQ and SPC models, respectively, for 256 water molecules and it becomes progressively more demanding as $O(N^2)$ with the increasing number of molecules compared to $O(N^{3/2})$ for the Ewald method.[12] Since we treat large systems with 2700 water molecules with or without salt ions, we adopt the nonpolarizable water model SPC/E combined with the Ewald method, which yields rather qualitative but reasonable results for electrostatic properties.

Complementary to the previous studies, we examine the heating of water by low-frequency microwaves in typical phases, including liquid water, ice, and dilute saline solution, by means of classical molecular dynamics simulations.[13] We use the microwaves in the 2.5–20 GHz frequency range and the field strength of $E_{\mathrm{rms}} \sim 0.01$ V/Å and a relatively large system containing 2700 water molecules. As we focus on the heating process in the low-frequency and low field strength regime, we adopt a fixed-point-charge, rigid-body model for water and a constant volume periodic system without an en-

ergy or particle reservoir. As for the diagnosis, we directly measure the kinetic and potential energies to obtain transferred energies from the microwaves.

We have confirmed that water in the liquid phase is heated by microwaves through the excitation of rotational motion of permanent electric dipoles of water molecules which is delayed from the wave electric field. The microwave energy is transferred to kinetic and internal (intermolecular) energies of water, where the energy stored as the internal one amounts to about one-third that of the total absorbed power. Dilute salt water is heated significantly more than pure water because of the Joule heating of salt ions, especially that of large-size Cl^- ions. On the other hand, the water in ice phase is hardly heated by low-frequency microwaves, since electric dipoles exhibit substantial directional inertia due to the rigid network of water molecules.

This paper is organized as follows. In the next section, the simulation method and parameters adopted in this study are described. In Sec. III, our simulation results of microwave heating are presented for three typical cases including ice, liquid water, and salt-added water. Section IV will be a summary of this paper.

II. SIMULATION METHOD AND PARAMETERS

To study the heating process of water, we use the microwaves of the frequency range 2.5–20 GHz, whose wavelengths and periods are 1.5–12 cm and 50–400 ps, respectively. These scale lengths are much larger than our model water system whose edge length is approximately 40 Å in one direction (typically one molecule resides in every 3 Å). Also, all the involved velocities are much less than the speed of light ($v/c \ll 1$). Under such circumstances, we can safely assume with the motion of water molecules and salt ions that the microwave is represented by spatially uniform, time-alternating electric field of the form

$$\tilde{E}_x(t) = E_0 \sin \omega t, \quad \tilde{B} = 0. \tag{1}$$

For the purpose of our study mentioned above, the water in liquid and ice phases is approximated by the assembly of three-point-charge rigid-body molecules known as the SPC/E model.[14] These molecules are placed in a constant volume cubic box. In this model, fractional charges δq are distributed at the hydrogen sites and $-2\delta q$ at the oxygen site, where $\delta q = 0.424|e|$ with e the electronic charge. The ith atom of the water molecule moves under the Coulombic and Lennard-Jones forces,

$$m_i \frac{d\mathbf{v}_i}{dt} = -\nabla \left\{ \sum_j \frac{q_i q_j}{r_{ij}} + 4\epsilon_{\mathrm{LJ}} \left[\left(\frac{\sigma}{r_{ij}} \right)^{12} - \left(\frac{\sigma}{r_{ij}} \right)^{6} \right] \right\}, \tag{2}$$

$$\frac{d\mathbf{x}_i}{dt} = \mathbf{v}_i, \tag{3}$$

where $\mathbf{r}_i$ and $\mathbf{v}_i$ are the position and velocity of the ith atom, respectively, $r_{ij} = |\mathbf{r}_i - \mathbf{r}_j|$, and m_i and q_i are its mass and charge, respectively. For the Lennard-Jones potential between interacting ith and jth atoms, the combination rules

$$\sigma = (\sigma_i + \sigma_j)/2, \quad \epsilon_{\mathrm{LJ}} = \sqrt{\epsilon_i \epsilon_j} \tag{4}$$

are used, where σ_i and ϵ_i are the diameter and Lennard-Jones potential depth of the ith atom, respectively. In Eq. (2), the Lennard-Jones force is calculated only for the oxygen atoms with $\sigma_{\mathrm{O}} = 3.17$ Å and $\epsilon_{\mathrm{LJ,O}} = 0.65$ kJ/mol. The length of the hydrogen-oxygen bond is 1.00 Å and the angle between these bonds is 109.47°. The constraint dynamics procedure called "Shake and Rattle algorithm"[15] is used to maintain these bond length and angle. Salt (Na^+Cl^-) is added in some runs. The Lennard-Jones forces are calculated for the pair of the ionic atom and oxygen atom of water molecules, where the diameter and the Lennard-Jones potential depth used for Na^+ are 2.57 Å and 0.062 kJ/mol, respectively, and those for Cl^- are 4.45 Å and 0.446 kJ/mol, respectively.

As for the initial conditions, we use highly structured crystal ice $\mathbf{I}_c$ with 14 molecules in all three directions under given densities of 1.00 g/cm^3 for liquid water (the edge length of the cubic box is fixed at $L = 43.448$ Å) and 0.93 g/cm^3 for ice ($L = 44.512$ Å). Thus, we have approximately 2700 water molecules in the box with periodic boundary conditions. Water molecules, especially those of ice and liquid water, form a three-dimensional network with hollow unit cells consisting of six-membered water rings.[16] The connection between the molecules is made by the hydrogen bond between a hydrogen atom and an adjacent oxygen atom that belongs to a different molecule. Each molecule donates two hydrogen bonds to adjacent molecules and accepts two hydrogen bonds from other molecules to form the hydrogen-bonded network; thus there is a freedom to which neighboring molecules the two hydrogen atoms are donated from one molecule. The initial orientations of water molecules are prescribed such that the directions of two hydrogen atoms bonded to an oxygen atom are swapped under the $\mathbf{I}_c$ symmetry until the sum of the bonded O–H vectors is nullified for each of all three directions; the number of water molecules in any direction must be an even number,[17] which is 14 for the system length of 44.512 Å. All simulation runs are preceded by an equilibration phase of 100 ps at given temperature and density before microwaves are applied.

The calculation of the Coulombic forces under the periodic boundary condition requires the charge sum in the first Brillouin zone and their infinite number of mirror images (the Ewald sum[18]). The sum is calculated with the use of the particle-particle, particle-mesh algorithm and the procedure of minimizing the rms error in the force.[19,20] We use $(32)^3$ spatial meshes and the third order spline interpolation for the calculation of the reciprocal space contributions to the Coulombic forces and take direct summations for the short-range particle-particle forces with the real-space cutoff of 10 Å and the Ewald screening parameter $\alpha = 0.25$ Å^{-1}. This yields the relative rms error in the force of 1.1×10^{-4}. We note that the accuracy of the Ewald sum can be optimized with the Lekner method for highly ionic environments.[21] The time integration step is $\Delta t = 1$ fs, for which the detection level of heating for liquid water is $(dW/dt)_{\mathrm{noise}} \sim 2 \times 10^{-5} kT_0$/ps. We use our personal computer (PC) cluster machines, each of which consists of four Pentium 4/EM64T (3.4 GHz) processors, and a 500 ps run takes typically 48 h.

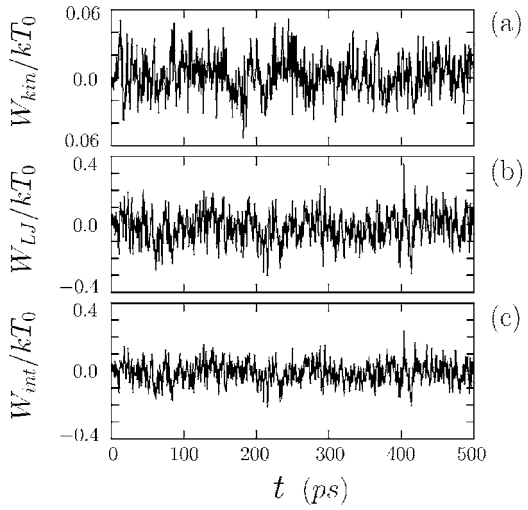

FIG. 1. The time history of (a) the average kinetic energy, (b) the average Lennard-Jones energy, and (c) the average intermolecular energy per molecule, for the ice at temperature of 230 K. Microwaves are applied for $t>0$, whose frequency is 10 GHz and its strength is 2.23×10^6 V/cm or $E_0p_0/kT_{300}\sim0.42$.

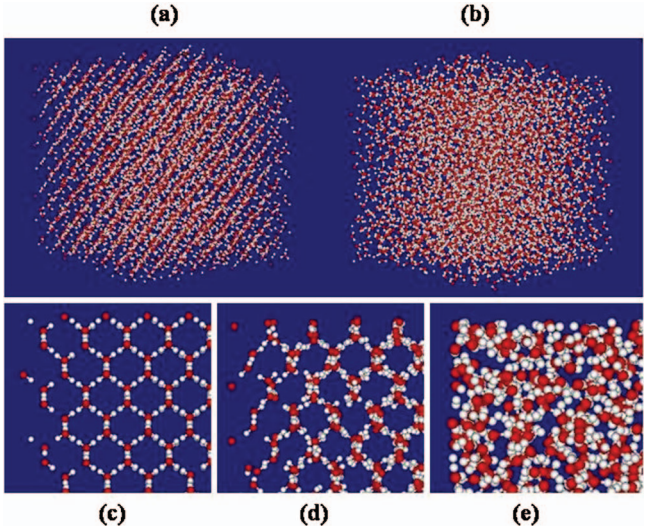

FIG. 2. (Color) The geometrical arrangement of water molecules at $t=500$ ps after the microwave application, for (a) the ice at 230 K and (b) liquid water initially at 300 K. Enlarged edge parts are shown for (c) the initial $\mathbf{I}_c$ ice, (d) the ice at 230 K [edge part of (a)], and (e) liquid water [edge part of (b)]. The microwave frequency is 10 GHz and its field strength E_0 is $E_0p_0/kT_0\sim0.42$ with $T_0=300$ K.

Three types of runs are performed, namely, (i) ice of the $\mathbf{I}_c$ form at 230 K, (ii) pure water whose initial temperature is 300 K, and (iii) salt water with 1 mol % NaCl (3.2 wt % or $0.57M$) starting at 300 K. In numerical simulations, we use large electric fields in order to detect heating in a reasonable computation time, which is typically $E_0\sim1\times10^6$ V/cm. Nevertheless, this is not a large electric field when viewed from water molecules, since the dipole energy $E_0p_0\sim4.8\times10^{-3}$ eV ($p_0\sim2.4\times10^{-18}$ esu cm is the electric dipole of our model water) is still less than thermal energy $kT_0\sim2.6\times10^{-2}$ eV at room temperature $T_0=300$ K, where k is the Boltzmann constant. The dipole energy is by orders of magnitude less than the hydrogen-bond energy of 2.5 eV per bond.

III. SIMULATION RESULTS

In the following sections, unless otherwise specified, we use the microwaves of the frequency 10 GHz (period 100 ps) and the strength $E_0=2.23\times10^6$ V/cm, which corresponds to the ratio of the dipole energy and thermal energy at $T_0=300$ K, $E_0p_0/kT_0\sim0.42$.

A. Heating of crystal ice

The microwave heating of water in ice phase is examined for the crystal ice $\mathbf{I}_c$ at the temperature of 230 K. Figure 1 shows the time history of average quantities: (a) the kinetic energy of water molecules $W_{\mathrm{kin}}=\langle\frac{1}{2}m\mathbf{v}^2\rangle$, which includes both translational and rotational energies, (b) the Lennard-Jones energy, $W_{\mathrm{LJ}}=\langle4\epsilon_{\mathrm{LJ}}[(\sigma/r_{ij})^{12}-(\sigma/r_{ij})^6]\rangle$, and (c) the intermolecular energy, which is the sum of the Lennard-Jones energy and the Coulombic energy $W_c=(1/N(N-3))\times\Sigma'_{ij}q_iq_j/r_{ij}$, where the prime means the summation excluding the charge pairs on the same molecule. The kinetic energy above is the index of heating, and the maximum and minimum of Fig. 1(a) correspond to 230±7 K, respectively.

Despite the microwave application for $t>0$, the kinetic and intermolecular energies remain nearly constant except for small periodic fluctuations.

The geometrical arrangement of water molecules is shown in Fig. 2 at the final time $t=500$ ps for (a) ice at 230 K, (b) liquid water initially at 300 K (to be mentioned in Sec. III B), and [(c)–(e)] their enlarged plots of the edge parts. The water in ice phase of Fig. 2(c) has a complete crystal structure, which remains nearly intact after the microwave application as seen in Figs. 2(d) and 2(a). The distribution functions of electric dipoles of water molecules for the ice in terms of the directional cosine,

$$\cos\Theta_i=\hat{x}\cdot\mathbf{p}_i/p_i, \tag{5}$$

are shown in Fig. 3, which also stay almost unchanged during the microwave application (the ordinate is in a logarithmic scale), where $\mathbf{p}_i(t)$ is the electric dipole of the ith molecule and $\hat{x}$ is the unit vector in the x direction. This immobility of electric dipoles is attributed to the rigidity of the network of water molecules due to hydrogen bonds. These observations indicate that pure crystal ice is not heated by microwaves of a few gigahertz frequency at the applied intensity. On the other hand, methane hydrate crystallites were found to be ruptured by microwave fields at higher intensities.[22]

B. Heating of liquid water

Now we examine the microwave heating of water in the liquid phase starting at the temperature of 300 K. In the cubic box there are 2744 water molecules which have been equilibrated without the microwave field at this temperature.

The depiction of molecular arrangement of Figs. 2(b) and 2(e) at $t=500$ ps after microwave application clearly shows that the water molecules in the liquid phase are randomized both in guiding center positions and molecular ori-

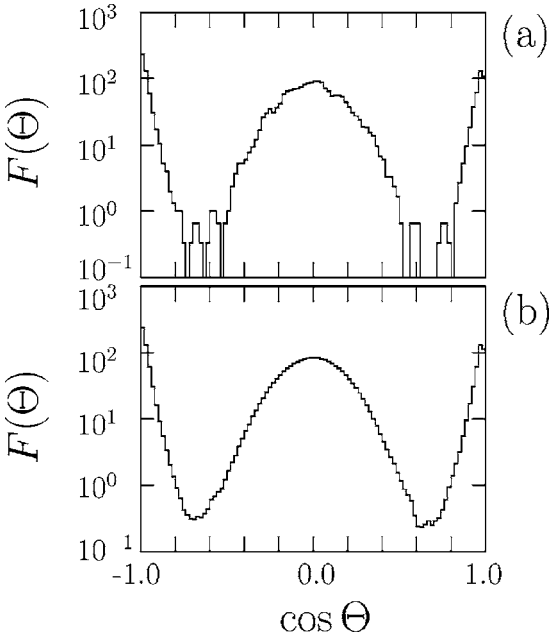

FIG. 3. The distribution of water electric dipoles as the function of the directional cosine cos Θ, Eq. (5), for the ice at temperature of 230 K shown in Fig. 1, (a) before (t=0) and (b) after (t=500 ps) the application of microwaves. The ordinates are in a logarithmic scale.

entations by absorbing microwaves. Figure 4 shows the time history of (a) the kinetic energy of water molecules, (b) the Lennard-Jones energy, and (c) the sum of the Coulombic and Lennard-Jones energies. When microwaves are switched on at t=0 in Fig. 4, the kinetic energy of water molecules begins to increase at a constant rate; the final temperature is 350 K. The average distance between the molecules is expanding during this rearrangement of molecules (the energy minimum of the Lennard-Jones potential is located at $r_{OO}=2^{1/6}\sigma_O=3.56$ Å). We note that the water at rest is in a minimum energy state because of strong attraction forces due to

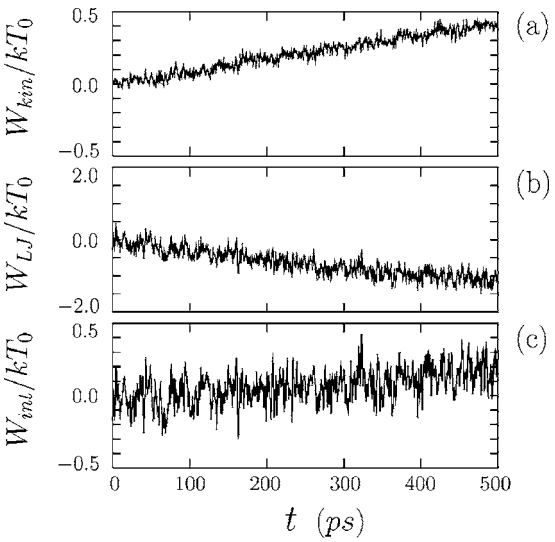

FIG. 4. The time history of (a) the average kinetic energy, (b) the average Lennard-Jones energy, and (c) the sum of average Coulombic and Lennard-Jones energies per molecule, for liquid water of initial temperature of 300 K. Microwave frequency is 10 GHz and its strength is $E_0p_0/kT_0 \sim 0.42$.

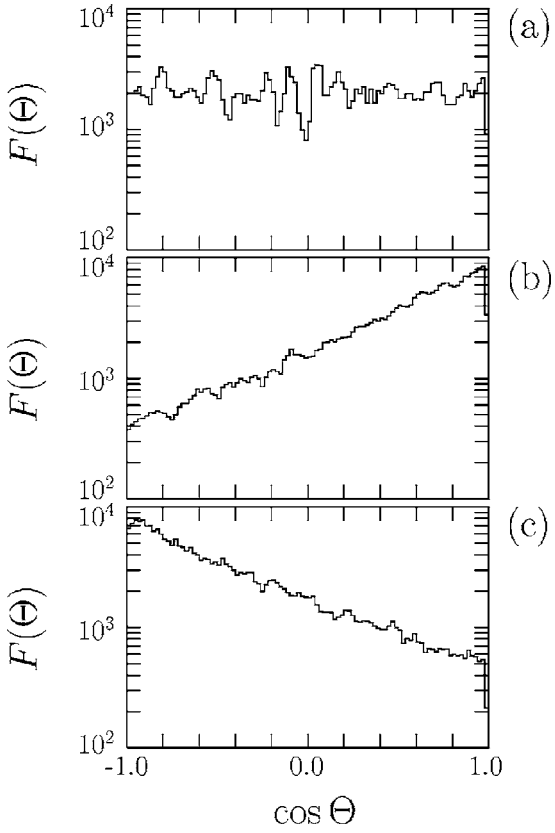

FIG. 5. The distribution of electric dipoles as the function of the directional cosine cos Θ, for (a) just before the application of microwaves (t=0), at (b) t=50 ps, and at (c) t=100 ps for liquid water initially at temperature of 300 K shown in Fig. 4. The ordinates are in a logarithmic scale.

hydrogen bonds. The decrease in the Lennard-Jones energy and the increase in the Coulombic energy take place simultaneously under the microwave field, but the latter is larger than the former; thus the intermolecular energy increases. The microwave energy is transferred to kinetic and intermolecular energies of water, where the latter is about 35% that of the total absorbed power, as seen by comparing Figs. 4(a) and 4(c).

The observed heating is attributed to the excitation of the rotational motion of permanent electric dipoles of water molecules and simultaneous energy transfer to translational energy via molecular collisions. Angular distributions of electric dipoles as the function of the directional cosine of their orientation are shown in Fig. 5 in 50 ps intervals. Before the microwave application, the electric dipoles in Fig. 5(a) have random orientations at room temperature. When the microwave electric field is present, the dipoles align along the direction of the time-alternating electric field $\tilde{E}$, as seen in Figs. 5(b) and 5(c). At each instant, the angular distribution of electric dipoles nearly follows the statistical (Boltzmann) distribution,

$$F(\Theta) \cong A^{-1} \exp[(\tilde{E}p \cos \Theta)/kT] \tag{6}$$

with regard to the angle Θ, where $\varepsilon_d=-\tilde{E}p \cos \Theta$ is the dipole energy and the normalization constant is $A=\int F(\Theta)\sin \Theta d\Theta=(kT/Ep)[\exp(kT/Ep)-\exp(-kT/Ep)]$.

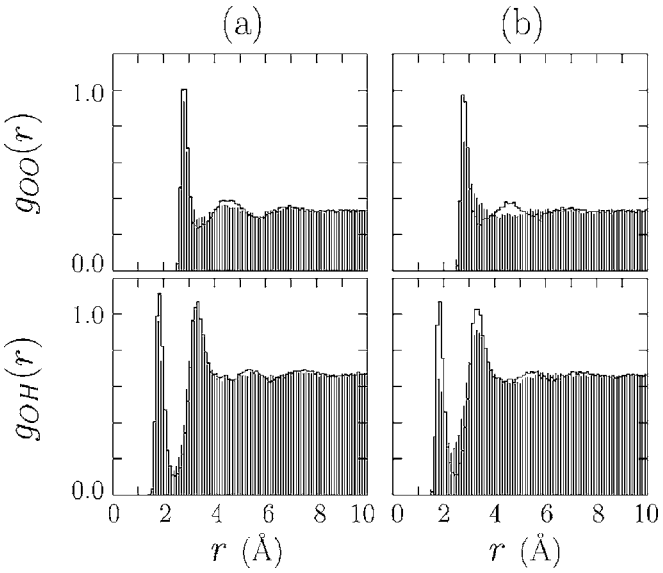

FIG. 6. The radial distribution functions (RDFs) of the oxygen-oxygen pairs $g_{OO}(r)$ and those of oxygen-hydrogen pairs $g_{OH}(r)$, for (a) liquid water at 300 K and (b) salt water with 1 mol % salinity. The initial RDFs are shown by solid lines and those at the final times [t=500 ps for (a) and t=1.4 ns for (b)] are shown by shaded histograms.

The radial distribution function (RDF) between oxygen atoms $g_{OO}(r)$ for liquid water in Fig. 6(a) reveals that the initial gap located at $r_{OO}\sim 3.5$ Å is filled after the microwave application. The gap at $r_{OH}\sim 2.5$ Å in the RDF between hydrogen and oxygen atoms, $g_{OH}(r)$, is also partially filled. These observations indicate the randomization of the orientation of electric dipoles and the increase in the distances between oxygen atoms. They are consistent with the increase in the Coulombic energy $\Sigma_{i>j}q_iq_j/r_{ij}$, where the major contribution comes form the hydrogen and oxygen pairs due to hydrogen bonds.

However, it should be noted that a finite phase difference is required between the orientation of electric dipoles of water molecules and the electric field for the energy to be transferred from microwaves to water. The sum of the x component of electric dipoles is obtained by

$$P_x = \int_{-\pi}^{\pi} p\cos\Theta F(\Theta)\sin\Theta d\Theta \cong \frac{p}{2}\int_{-1}^{1}\cos\Theta\left[1+\frac{Ep}{kT}\cos\Theta\right]d\cos\Theta = \left(\frac{Ep}{3kT}\right)p, \tag{7}$$

where we have used Eq. (6) and expanded it assuming $Ep/kT \ll 1$ [the next order term is $(p/15)(Ep/kT)^3$, which is a few percent of the above leading term even for $Ep/kT\sim 0.4$]. Then, we put the electric dipole $p(t)=p_0\sin(\omega(t-\tau))$ with the phase lag τ. The work done to the dipoles at the position x per unit time by the electric field Eq. (1) is

TABLE I. The heating and energy absorption rates of liquid water, ice, and saline solution at various initial temperatures, with experimentally measured dielectric losses as references. The microwave frequency in numerical simulations is 10 GHz, the electric field strength is $E_0=2.23\times 10^6$ V/cm (or $E_0p_0/kT_0\sim 0.42$), and the heating and absorption rates are in the units of kT_0/ps molecule, with $T_0=300$ K. The dielectric losses by experiments are ϵ''/ϵ_0 for 2.45 GHz and 25 °C.

State	Temperature (K)	Heating rate	Absorption rate	Experiments
Ice	230	Very small	Very small	<0.01
Water	300	7.6×10^{-4}	1.1×10^{-3}	13
Water[a]	400	2.6×10^{-4}	4.7×10^{-4}	2.4[b]
Salt water[c]	300	1.7×10^{-3}	3.0×10^{-3}	18[d], 42[e]

[a]Hot water in the liquid phase (due to a constant volume).
[b]95 °C (Ref. 4).
[c]1 mol % NaCl salt concentration.
[d]1.0 mol % salinity (6 GHz) (Ref. 26).
[e]0.5 mol % salinity (3 GHz) (Ref. 4).

$$\frac{dW_E}{dt} = \left\langle E\frac{dP_x}{dt}\right\rangle = \frac{(p_0E_0)^2}{3kT}\left\langle \sin\omega t\frac{d}{dt}\{\sin\omega t\sin^2(\omega(t-\tau))\}\right\rangle = \frac{(p_0E_0)^2}{24kT}\omega\sin 2\omega\tau. \tag{8}$$

If we assume the Debye-type relaxation $\tau\cong\zeta/2kT$ and $\omega\tau \ll 1$, where ζ is the friction from adjacent water molecules,[23] then we have

$$\frac{dW_E}{dt} \cong \frac{1}{24}\zeta\omega^2\left(\frac{p_0E_0}{kT}\right)^2. \tag{9}$$

This formula indicates that, without friction $\zeta=0$, the phase lag vanishes $\tau=0$; thus we have no microwave heating of water.

The heating and energy absorption rates of liquid water at 300 K by the microwaves of $f=10$ GHz and $E_0=2.23\times 10^6$ V/cm are $dW/dt\sim 7.6\times 10^{-4}\ kT_0$/ps and $1.1\times 10^{-3}\ kT_0$/ps, respectively, as listed in Table I. The expected energy absorption rate using the experimentally obtained imaginary part of the dielectric constant $\epsilon''/\epsilon_0\cong 13$ becomes $2\pi f\epsilon''E_0^2/8\pi n_0\sim 5.4\times 10^{-5}$ erg/ps molecule $=1.3\times 10^{-3}\ kT_0$/ps molecule by von Hippel,[4] where $n_0\cong 3.3\times 10^{22}$ molecules/cm^3 is the density of water molecules. This estimate is in fair agreement with the simulation value of the energy absorption rate shown in Table I. Further, by equating Eq. (8) and the energy absorption rate in the simulation, then we have the estimate for the phase lag as $\tau\sim 19$ ps.

The total energy absorption rate by the water system may be obtained by integrating the local energy absorption rate over the depth (x coordinate). Since the wave electric field attenuates as $E(x)=E(0)\exp(-x/\lambda)$ in dielectric medium, then we have

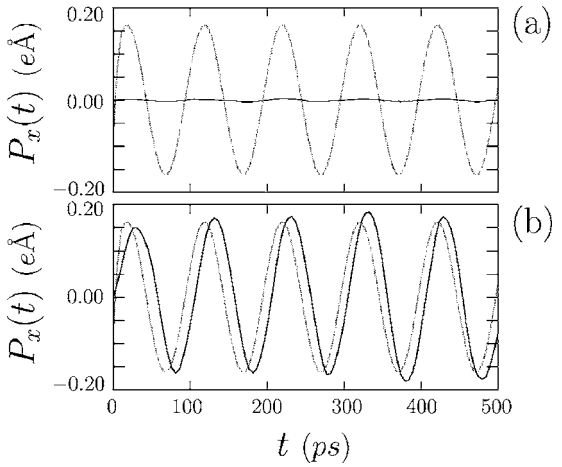

FIG. 7. The x component of the average electric dipole $\langle P_x(t)\rangle=\Sigma_i \mathbf{P}_i\cdot\hat{x}/N$ and the microwave electric field $E_x(t)$ (gray lines) for (a) the ice at 230 K shown in Fig. 1 and (b) liquid water initially at 300 K shown in Fig. 4.

$$\int_0^{\ell} dx = \lambda \int_{E_{\min}}^{E(0)} dE/E, \tag{10}$$

where $E_{\min}=E(0)\exp(-\ell/\lambda)$ and $E(0)$ is the electric field at the interface (inside) of water. The length λ is a few centimeters for 2–10 GHz microwave in water. For the power dependence on the electric field $\dot{W}_E \sim E^{\alpha}$, the integration yields the same power dependence even when $\ell \geqslant \lambda$ by substituting E_0 of the local formula by $(\lambda/\ell(\alpha-1))E(0)$.

Existence of the phase lag is verified in Fig. 7 which shows the temporal phase variations of the x component of the average water electric dipole $P_x(t)$ and the electric field, for (a) ice at 230 K and (b) liquid water initially at 300 K. For the ice case, variations of the electric dipoles are very small. For the liquid water, on the other hand, we see large oscillations in the x component of electric dipoles. Their amplitude is almost the value expected by Eq. (7), and a finite phase difference exists between the electric dipole and the electric field. The phase lag of electric dipoles from the microwave electric field is about 12 ps on average. This is about two-thirds that of the phase lag obtained above using Eq. (8) but is close to the rotational relaxation time of 8 ps of water dipoles at 25 °C and a fraction of the macroscopic relaxation time 40 ps (25 GHz) of bulk water.[24]

The dependence of the energy transfer rate to liquid water on the strength of the microwave electric field is shown in Fig. 8, for the temperature of 300 K and the wave frequency of 10 GHz. Here, the time rate of the increase in the kinetic energy is plotted by filled circles, and that in the total energy (the sum of the kinetic and intermolecular energies) is plotted by open circles, with both axes in logarithmic scales. These two energy transfer rates from the microwaves increase by power laws of the microwave electric field and are scaled as

$$\left(\frac{dW}{dt}\right)_{\text{wat}} \propto E^{\alpha}, \tag{11}$$

with $\alpha \cong 2.0$ both for the wave power absorbed by the water system and the kinetic energy of water. We note that about

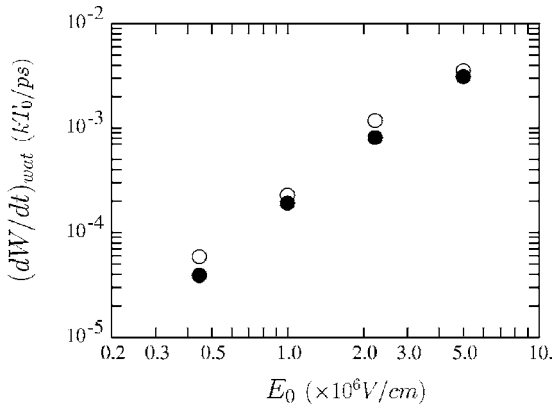

FIG. 8. The dependence of the energy transfer rate from microwaves to liquid water (initially at 300 K) on the strength of microwave electric field is shown for the kinetic energy dW_{kin}/dt (filled circles), which corresponds to heating of water, and the system total energy dW_{sys}/dt (open circles), which includes the kinetic and intermolecular energies. The microwave frequency is 10 GHz. The data points are well fitted by power laws, Eq. (11).

30% of the absorbed microwave energy is stored as the intermolecular energy to rearrange water molecules. These dependences on the electric field agree with that given by Eq. (9).

The dependence of the energy transfer rate on the frequency of microwaves is shown in Fig. 9, where the frequency is in the $f=\omega/2\pi=2.5$–20 GHz range. The transferred energy from the microwaves increases with the wave frequency and is scaled by

$$\left(\frac{dW}{dt}\right)_{\text{wat}} \propto \omega^{\beta}, \tag{12}$$

with $\beta \cong 1.5$ both for the total energy absorbed by the water system and for the kinetic energy of water molecules. These frequency dependences are somewhat weaker than that of the formula Eq. (9), as the approximation $\sin 2\omega\tau \cong 2\omega\tau$ may deteriorate at high frequencies.

In Table I, the heating rates that we have measured by numerical simulations of the ice and liquid water at two initial temperatures are listed, together with that for the salt

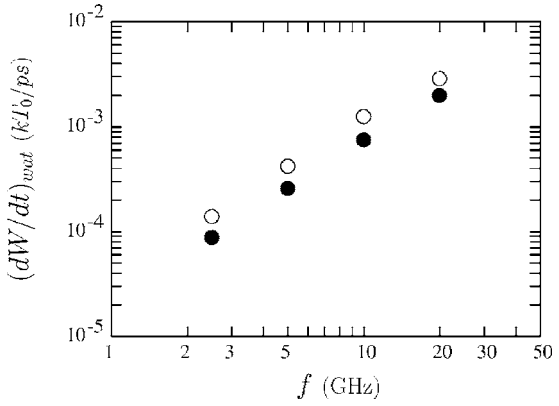

FIG. 9. The dependence of the energy transfer rates from microwaves to liquid water (initially at 300 K) on the frequency f (GHz) of microwaves is shown for the kinetic energy dW_{kin}/dt (filled circles) and for the system total energy dW_{sys}/dt (open circles). The electric field strength is 2.23×10^6 V/cm (or $E_0 p_0/kT_0 \sim 0.42$). The data points are well fitted by the power laws, Eq. (12).

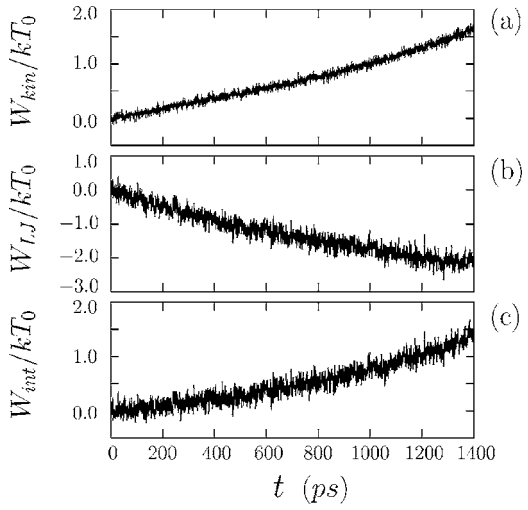

FIG. 10. The time history of (a) the average kinetic energy, (b) the average Lennard-Jones energy, and (c) the sum of average Coulombic and Lennard-Jones energies per molecule, for salt water with 1 mol % NaCl salinity initially at temperature of 300 K. Microwave frequency is 10 GHz and its strength is $E_0p_0/kT_0 \sim 0.42$.

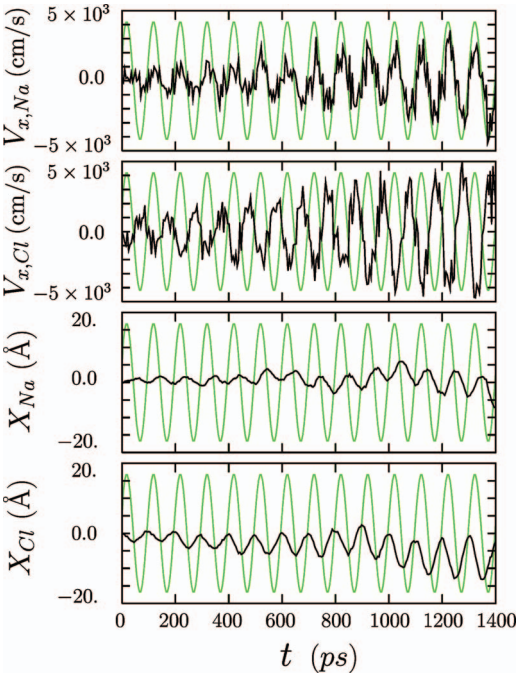

FIG. 11. (Color) The time history of the average x-component velocity of Na^+ and Cl^- ions and that of the average positional shift of Na^+ and Cl^- ions in the x direction (from top to bottom), for the run shown in Fig. 10. Green lines are the amplitude of the applied electric field.

water (to be mentioned in Sec. III C). The heating rate for the ice is below our detection level. The heating rate of hot water at 400 K (in liquid phase because of the constant volume) is small and only a fraction in comparison with that at room temperature. This is due to less friction at higher temperatures, since the intermolecular distances of water molecules become large. The simulation value is consistent with the experiment.[4]

C. Heating of salt water

We examine the heating process of dilute saline solution, which corresponds to our daily applications including the heating of salty food in a microwave oven. In the simulation, we place 27 Na^+ and 27 Cl^- ions (1 mol % NaCl or 3.2 wt % salinity) at random positions to the water system at room temperature. The number of water molecules of 2717 here is less than that of the pure water case with the same volume to avoid overlap of salt ions and water molecules. We equilibrate the solution for 100 ps before the microwave application at $t=0$.

Figure 10 shows the time history of salt water heating by microwaves of 10 GHz and the field strength of 2.23×10^6 V/cm ($E_0p_0/kT_{300} \sim 0.42$). The kinetic energy of water molecules increases only slightly faster (11%) than for pure water in the early stage. After a waiting time of 0.8 ns, a rapid heating phase sets in and the salt water is heated by a few times more than the pure water. The length of this microscopic waiting time among the runs with different microwave field strengths is not indexed to the water temperature at which the rapid heating sets in. The microwave power is absorbed also as the intermolecular energy, which is comparable to the increase in the kinetic energy [Fig. 10(c)].

The behavior of salt ions in saline solution after the microwave application is shown in Fig. 11. Both the cations and anions are accelerated by the electric field, and the maximum values of their average velocities expand continuously in time. Their field-induced motions are nearly in phase and out of phase with the microwave field for cations and anions, respectively. Interestingly, the degree of acceleration is appreciably larger for the heavier and larger anions than cations. This fact may be due to that small-size cations are well contained in the water network compared with anions whose diameter is comparable to the cell size of the network (this point is to be mentioned in the RDF of salt ions in Fig. 12). The mean displacements of salt ions in Fig. 11 show that anions drift toward the negative x direction and its amplitude is larger than that of cations which drift to the positive x direction. We note that the amount of the positional shift for anions increases linearly up to $t=0.8$ ns. At the end of this period when the rapid hating phase begins, the average positional shift for anions is roughly 7 Å which is comparable to the unit cell size of the water network consisting of hydrogen-bonded six-membered rings. This implies that the rapid heating of saline solution is connected with the field-induced motion of anions in the water network (this point will be verified later in this section).

The distribution function of the velocities in the x direction (along the microwave electric field) and those in the y and z directions have been examined for salt ions in Fig. 11. In the solids such as zeolites and titanium oxides, athermal kinetic energy distribution was seen for ions.[21,25] For salt ions in water, the velocity distribution function consists of a single Boltzmann distribution in all three directions under the present wave frequency and intensity. The salt temperature in the direction of the electric field T_x is slightly higher than those in other directions $T_\perp=(T_y+T_z)/2$, and their ratio appears to level off at $(T_x/T_\perp)_{\text{salt}} \cong 1.2$ in the late stage of Fig. 11. However, no such anisotropy is found for water temperatures; $(T_x/T_\perp)_{\text{water}} \cong 1.0$ throughout the same run.

The radial distribution functions (RDFs) of oxygen-

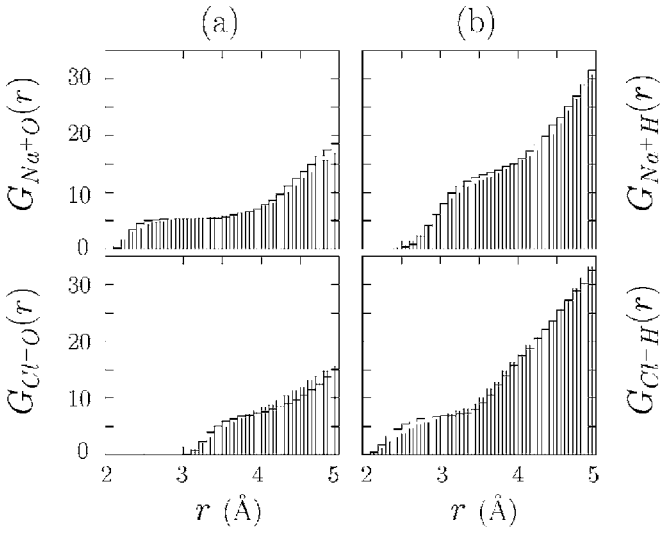

FIG. 12. The accumulated radial distribution functions of Na^+ (top row) and Cl^- ions (bottom row) with respect to (a) oxygen atoms and (b) hydrogen atoms, for the initial time $t=0$ (solid line) and after the microwave application at $t=1.4$ ns (shaded histogram) for the salt water shown in Fig. 10. Microwave frequency is 10 GHz and its strength corresponds to $E_0p_0/kT_0 \sim 0.42$.

oxygen pairs, $g_{OO}(r)$, and those of oxygen-hydrogen pairs, $g_{OH}(r)$, are shown for the above salt water in Fig. 6(b). Initial RDFs are shown by solid lines and those at the final times are shown by shaded histograms. We see drastic differences between the RDFs before and after the microwave application. The heights of the first peak at 1.9 Å in $g_{OH}(r)$ and that at 2.8 Å in $g_{OO}(r)$ are much reduced, and the gaps between the first and second peaks are filled. This reveals the randomization of the position and orientation of water molecules, and thus weakening of the water network.

The accumulated RDF for the oxygen-hydrogen pairs at the initial time has a flat pedestal, from which the association number of a hydrogen atom to oxygen atoms is approximately 2 at $r \cong 2$ Å. At $t=1.4$ ns, the inner edge of the accumulated RDF is receded for oxygen-hydrogen pairs. The accumulated RDF of the Na^+ ions, $G_{Na^+O}(r)$, in Fig. 12 shows that they are associated with five oxygen atoms at $r \sim 2.5$ Å which changes only slightly during the microwave application. This means that Na^+ ions are well contained in the unit cell of the water network, as previously mentioned. On the other hand, $G_{Cl^-O}(r)$ shows that a Cl^- ion is loosely associated with seven oxygen atoms at $r \cong 3.8$ Å. After the microwave application at $t=1.4$ ns, the inner edges of the accumulated RDFs for Cl^- ions, $G_{Cl^-O}(r)$ and $G_{Cl^-H}(r)$, recede both with respect to oxygen and hydrogen atoms. This implies that large Cl^- ions are constantly pressed by water molecules and are less stably trapped in the water network. As has been suggested by Fig. 11, oscillating Cl^- ions are generating friction against water molecules and deteriorating the hydrogen bonding between them.

The heating rates of the saline solution with 1 mol % NaCl in the present molecular dynamics simulations and that of experiments are also listed in Table I. The experimental values are very diverse probably because of the different experimental devices and sample sizes. The old experiments were made with a Pt foil-wrapped resonator in which

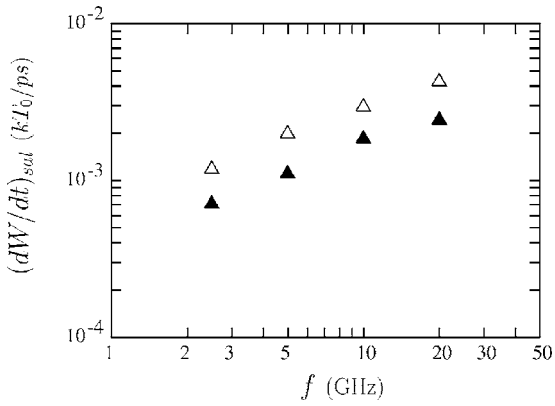

FIG. 13. The dependence of the energy transfer rate from microwaves to salt water with 1 mol % salinity on the frequency f (GHz) of microwaves is shown for the kinetic energy dW_{kin}/dt (filled triangles) and for the system total energy dW_{sys}/dt (open triangles). The electric field strength is 2.23×10^6 V/cm, which corresponds to $E_0p_0/kT_0 \sim 0.42$.

samples were placed.[4] Another measurement was done with a cavity resonator using two microwaves of different frequencies, one for heating and the other for measurement.[26] The heating rate of salt water in the simulation ($t>1$ ns) is just between the experimental values.

The dependence of the energy transfer rate from microwaves to salt water on the frequency of microwaves is shown in Fig. 13. Both the energy transfer rates to the system (open triangles) and that to the kinetic energy of water (filled triangles) are scaled as

$$\left(\frac{dW}{dt}\right)_{\text{salt}} \propto \omega^{\gamma}, \tag{13}$$

with $\gamma \cong 0.6$, which is less sensitive to the microwave frequency than for pure water. We expect that the heating of salt water is not attributed to a simple acceleration of salt ions but is the result of the interactions between charged salt ions and the water network.

Although salt ions and water molecules interact toward equilibration, we can separate the microwave energy going via the salt ions and that absorbed directly by water molecules. The measurement of the energy transfer rates $\mathbf{E}\cdot\mathbf{J}_{\text{salt}}$ and $\mathbf{E}\cdot d\mathbf{P}/dt$ gives the microwave energies absorbed through the salt and water dipole channels, respectively, where $\mathbf{J}_{\text{salt}} = \Sigma_i q_i \mathbf{v}_i$ is the current carried by salt ions. The time-integrated values of these terms increase monotonically in time with small fluctuations corresponding to half the wave period. The ratio of the energy transfer rates becomes $|\mathbf{E}\cdot\mathbf{J}_{\text{salt}}|/|\mathbf{E}\cdot d\mathbf{P}/dt| \cong 2.1$ in the late stage of salt water heating shown in Fig. 10. Large salt ions Cl^- contribute to 65% of the $\mathbf{E}\cdot\mathbf{J}_{\text{salt}}$ term. Thus, despite the diluteness of the saline solution of 1 mol %, more microwave energy is absorbed through the salt channel than the dipole channel.

The aforementioned statement is supported by the runs with special saline solutions, (i) heavy salt ions, (ii) small Cl ions $\sigma_{Cl^-}=\sigma_{Na^+}=2.57$ Å, and (iii) *noncharged* salt, and then apply the microwaves of 10 GHz frequency and the strength $E_0=2.23\times10^6$ V/cm. In case (i), the salt ions are made ten times as heavy as their original masses; thus their vibrations are slower and smaller than the normal salt. The heating rate

of water is found to be $dW_{\rm kin}/dt \sim 1.5\times10^{-3}kT_0/{\rm ps}$, which is similar to that of the normal salt water shown in Table I. For case (iii), the heating rate is small, $dW_{\rm kin}/dt \sim 7.1\times10^{-4}kT_0/{\rm ps}$, and this is almost the same as that of the pure water. This reveals that a noncharged sphere does not actively interact with water molecules. An interesting case is the small salt ions of (ii), for which the heating rate is intermediate between those of the pure and salt waters, $dW_{\rm kin}/dt \sim 9.9\times10^{-4}kT_0/{\rm ps}$. These special runs clearly indicate that large-size, charged ions such as Cl^- are playing important roles in the water heating process. Namely, large salt ions that do not fit in the unit cell of the water network make defects to it and cleave the network through oscillations in response to the microwave electric field.

IV. SUMMARY

In this paper, we have studied the heating process of liquid water, ice, and dilute saline solution by microwaves of 2.5–20 GHz, where molecular dynamics simulations are performed with the explicit point-charge, rigid-body water model. We have verified that water in the liquid phase is heated via the rotational excitation of water electric dipoles, which is delayed from the microwave electric field. Microwave energy is transferred to both kinetic and intermolecular energies of water, where the former corresponds to the heating of water and the latter is stored internally to rearrange water molecules. The latter energy occupies about one-third of the total absorbed microwave power.

Hot water is significantly less heated than the water at room temperature, because the electric dipoles follow the microwave field with less phase lags due to less friction. Water in ice phase is scarcely heated because the electric dipoles cannot rotate due to a tightly hydrogen-bonded network of water molecules. Dilute saline solution is significantly more heated than pure water. This is due to rapid heating of salt ions, especially that of large salt ions Cl^-, through field-induced motion by the microwave electric field and energy transfer by the interactions between salt ions and water molecules.

We remark that the microwave electric field in usual applications may be several orders of magnitude smaller than that used in the present study. The actual microwave field within the experimental sample should be considerably small compared with the surrounding vacuum space, because microwaves attenuate in the dielectric medium. If we assume that the strength of the microwave electric field is 10 V/cm (700 W microwaves correspond to the electric field of 730 V/cm, which becomes $1/\epsilon(3\ {\rm GHz}) \cong 1/77$ in water[4]) and the wave frequency is 2.5 GHz, then using the scalings Eqs. (11) and (12) we have

$$\frac{dW_{\rm kin}}{dt} \cong 1.8\times10^{-3}kT_0/{\rm s} \tag{14}$$

for the heating rate of water, where $T_0=300$ K. This corresponds to the temperature increase of roughly 70° in 2 min, which is consistent with our daily experiences.

We have two other remarks: (i) For the microwave of small intensity, several orders of magnitude more wave periods are required to heat water and related materials. (ii) A part of the energy stored internally may be released as heat in a long time scale, but it is beyond the scope our present study. Finally, the energy associated with the electric dipole ($\mathbf{E}\cdot\mathbf{p}$) in the presence of microwaves in our simulation is not exceeding thermal energy or hydrogen-bond energy of water molecules. Therefore, except for secondary phenomena such as a long-time relaxation of water structures, our simulations are correctly reproducing the essence of the microwave heating process of water and saline solution.

ACKNOWLEDGMENTS

One of the authors (M.T.) thanks Professor I. Ohmine and Dr. M. Matsumoto for fruitful discussions and for providing the $\mathbf{I}_c$ ice generating program. This work was supported by Grant-in-Aid Nos. 16032217 (2003–2005) and 18070005 (2006–2010) from the Ministry of Education, Science and Culture of Japan. The present simulations were performed using our LINUX-based PC cluster machines comprising of Pentium 4/EM64T and Opteron 275 processors.

[1] A. Stadler and C. O. Kappe, J. Chem. Soc., Perkin Trans. 2 **2000**, 1363; G. Horais, S. Pichler, A. Stadler, W. Gossler, and C. O. Kappe, Fifth Electronic Conference on Synthetic Organic Chemistry, 2001 (unpublished).
[2] G. Caliendo, F. Fiorino, E. Perissutti, B. Severino, S. Gessi, E. Cattabriga, P. A. Borea, and V. Santagada, Eur. J. Med. Chem. **36**, 873 (2001).
[3] R. D. Peelamedu, M. Fleming, D. K. Agrawal, and R. Roy, J. Am. Ceram. Soc. **85**, 117 (2002).
[4] *Dielectric Materials and Applications*, edited by A. R. von Hippel (MIT Press, Cambridge, MA, 1954), p. 361.
[5] S. Havriliak and S. J. Havriliak, *Dielectric and Mechanical Relaxation in Materials: Analysis, Interpretation, and Application to Polymers* (Hanser, Munchen, Germany, 1997).
[6] U. Kaatze and V. Uhlendorf, Z. Phys. Chem., Neue Folge **126**, 151 (1981); U. Kaatze, J. Chem. Eng. Data **34**, 371 (1989).
[7] T. Yamaguchi, S. H. Chong, and F. Hirata, J. Chem. Phys. **116**, 2502 (2002).
[8] C. Vega, E. Sanz, and J. L. F. Abscal, J. Chem. Phys. **122**, 114507 (2005).
[9] N. J. English and J. M. MacElroy, J. Chem. Phys. **118**, 1589 (2003).
[10] N. J. English and J. M. MacElroy, J. Chem. Phys. **119**, 11806 (2003).
[11] N. J. English, Mol. Phys. **104**, 243 (2006).
[12] N. J. English, Mol. Phys. **103**, 1945 (2005).
[13] Y. Rabin and M. Tanaka, Phys. Rev. Lett. **94**, 148103 (2005).
[14] H. Berendsen, J. Grigera, and T. Straatsma, J. Phys. Chem. **91**, 6269 (1987).
[15] H. C. Andersen, J. Comput. Phys. **52**, 24 (1983).
[16] M. Matsumoto, S. Saito, and I. Ohmine, Nature (London) **416**, 409 (2002).
[17] Initial configuration of ice is courtesy of Dr. M. Matsumoto.
[18] P. P. Ewald, Ann. Phys. **64**, 253 (1921).
[19] J. W. Eastwood and R. W. Hockney, J. Comput. Phys. **16**, 342 (1974).
[20] M. Deserno and C. Holm, J. Chem. Phys. **109**, 7678 (1998).
[21] N. J. English, D. C. Sorescu, and J. M. MacElroy, J. Phys. Chem. Solids **67**, 1399 (2006).
[22] N. J. English and J. M. MacElroy, J. Chem. Phys. **120**, 10247 (2004).
[23] W. T. Coffey, Y. P. Kalmykov, and J. T. Waldron, *The Langevin Equation with Applications in Physics, Chemistry and Electrical Engineering* (World Scientific, Singapore, 1996).
[24] I. Ohmine, J. Phys. Chem. **99**, 6767 (1995).
[25] C. Blanco and S. M. Auerbach, J. Phys. Chem. B **107**, 2490 (2003).
[26] H. Fukushima, Y. Yamanaka, and M. Matsui, J. Soc. Precis. Eng. **53**, 743 (1987).